Electron Observations in the Solar Wind and Magnetosheath

J. D. SCUDDER

Laboratory for Extraterrestrial Physics, NASA Goddard Space Flight Center Greenbelt, Maryland 20771

D. L. LIND

Astronaut Office, NASA Manned Space Flight Center Houston, Texas 77058

K. W. OGILVIE

Laboratory for Extraterrestrial Physics, NASA Goddard Space Flight Center Greenbelt, Maryland 20771

Observations made by a triaxial electron analyzer on the Ogo 5 spacecraft are presented and discussed. These cover a wide variety of solar-terrestrial conditions and took place in the interplanetary medium as well as in the magnetosheath. In the interplanetary medium, observations made on bow shock connected lines of magnetic force have been separated from those made on non-bow-shock connected lines. In general, sustained differences in temperatures derived from electrons with energies below 95 ev are of the order of a few percent, but at times greater temperature differences are observed. The mean temperature observed is $1.55 \pm 0.03 \times 10^5$ °K, and the mean temperature anisotropy is 1.18 ± 0.10, in general agreement with earlier work. A period when the plasma became nongyrotropic, associated with a mesoscale interplanetary electron temperature gradient of 8.5×10^5 °K/AU, was observed. Thirty-four bow shock crossings were observed, indicating mean density and temperature jumps of $\simeq$2.1:1 and 4.2:1, respectively. Velocity distribution functions f display a flat-topped form throughout the dawn part of the magnetosheath, and an asymmetry in f observed there is consistent with an energy flux in the sheath along the spacecraft-earth direction. Attempts to observe the temperature and density variations predicted by hydromagnetic theory along the spacecraft track in the magnetosheath were inconclusive.

Observations of solar wind electrons have been made on Pioneer, Explorer, Vela, and Ogo spacecraft. Determinations of electron temperatures have been reported by *Wolfe and McKibben* [1968], *Wolfe et al.* [1967], *Montgomery et al.* [1968, 1972], *Montgomery* [1972], and *Serbu* [1972]. However, the duration for which reliable electron temperatures are available is very small in comparison with that for which information on the ionic component is published.

We present from Ogo 5 data information derived from 25,626 electron temperature observations in the solar wind and a similar number of observations in the magnetosheath. The solar wind temperatures have an estimated absolute maximum error of 30%, and the relative error between individual determinations is of the order of 3%. These results show agreement in the mean with the Vela results reported by *Montgomery et al.* [1968] and *Montgomery* [1972]. With the availability of the vector magnetic field measured on the same spacecraft we can look in some detail at the dependence of electron thermal properties as a function of the local field geometry. This is of interest in view of activity upstream of the earth's bow shock reported by *Frank and Shope* [1968], *Fairfield* [1969], *Fredricks et al.* [1971], *Asbridge et al.* [1968], and *Ogilvie et al.* [1971]. In addition, we present 34 observations of electron temperature and density discontinuities across the bow shock. We have also observed the distribution function and mapped the temperature and density variation in a part of the dawn magnetosheath.

OGO 5 ELECTRON SPECTROMETER DESCRIPTION

The present observations were made with the Goddard Space Flight Center (GSFC) Ogo 5 triaxial electron spectrometer. The three individual analyzers, each with its own independent detector, were mounted with their axes mutually orthogonal on the attitude-controlled spacecraft. The body z axis of the spacecraft was always directed toward the earth. Each detector axis lies along an edge of a tetrahedron; the z axis was symmetrically situated with respect to the detector axes.

The electrostatic analyzers sampled an electron spectrum with 15 differential intervals between $E_{step} = 10$ ev and $E_{step} = 9.9$ kev every 23 sec and had nominal fields of view of $10° \times 10°$. The differential energy acceptance $\Delta E = 0.16\ (E_{step}\ (\text{ev}) + 100\ \text{ev})$.

TRANSFER FUNCTION

Electrons were accelerated before entering the analyzer [*Lind and McIlwraith*, 1966]; the acceleration resulted in a differential dependence of the solid angle of acceptance on particle energy. The transfer function describing this [*Scudder*, 1972] was used to convert the measured fluxes into fluxes per unit solid angle, and these were transformed into the coordinate frame moving with the plasma by using bulk speeds supplied by J. Binsack (private communication, 1971) as simultaneously determined by the appropriate MIT plasma probes on Explorer 33 and 35.

TEMPERATURES AND ANISOTROPIES

Electron temperatures in the solar wind were determined by fitting a Maxwellian velocity distribution function to the transformed fluxes for the 10-, 25-, 45-, and 80-ev channels. The major source of errors in the temperature determinations, which depend on the relative fluxes per unit solid angle in a given spectrum, is the convolution with the instruments transfer function. Although the thermal speed is much greater than the bulk speed, the transformation mentioned above results in a first-order correction to the temperature.

By T_e we mean $\frac{1}{3}\sum_{j=1,3} T_{ej} = \frac{1}{3}\,\mathrm{Tr}\,\mathbf{T}$, where T_{ej} is determined from the solar wind observations from the jth detector. We assume that there is a temperature ellipsoid, determined by $T(\theta,\phi)$, where θ and ϕ are the polar coordinates of a sensor with respect to the instantaneous vector magnetic field, and that the plasma is gyrotropic. This assumption requires $\frac{1}{3}\,\mathrm{Tr}\,\mathbf{T} \equiv (2T_\perp + T_\parallel)/3$ be equal, within experimental errors, to T_e. Conversely, if T_e does not lie between $T_\parallel$ and $T_\perp$, one or both of the assumptions about the symmetry of the distribution and its relation to the magnetic field direction have broken down.

Since the spacecraft had a fixed orientation in space, $T_\parallel$ and $T_\perp$ were computed by assuming a locally and instantaneously cylindrically symmetrical ellipsoid and rotating the temperature vectors obtained by the three detectors into any common plane containing the magnetic field. The two temperature determinations most widely separated in angle in the common plane were then used to estimate the semimajor and semiminor axes of the ellipse on which they were assumed to lie, unless the angle between the vectors was $<30°$, in which case no estimates were made. This procedure normally yields values of $T_\parallel$ and $T_\perp$ and an anisotropy estimate every 23 sec. If T_e did not lie between $T_\parallel$ and $T_\perp$ for the same time interval, we concluded our assumption of a gyrotropic plasma to be incorrect for that interval.

In view of the non-Maxwellian velocity distribution in the sheath we evaluate kinetic densities and temperatures defined by

$$\bar{N}_{sh} = \frac{4\pi}{3}\left(\sum_i n_{sh_i}\right)$$

$$\bar{T}_{sh} = \frac{m_e}{3k_B}\left(\sum_i t_{sh_i}\right)/\left(\sum_i n_{sh_i}\right)$$

where

$$n_{sh_i} \equiv \int f(v,\ \theta_i,\ \phi_i)v^2\,dv$$

$$t_{sh_i} \equiv \int f(v,\ \theta_i,\ \phi_i)v^4\,dv$$

to give a measure of the density and the internal energy in the magnetosheath.

FIELD LINE GEOMETRIES AND BOW SHOCK ACTIVITY

To evaluate the effects, if any, associated with field line connection to the shock surface, we have divided our data into sets for which

the line of force through the observer's position either 'misses' or 'hits' the bow shock.

We assume the bow shock to be represented by a hyperboloid of revolution of one sheet and that this surface is symmetrical about the aberrated earth-sun line. We further assume that its response to variations of solar wind flux is confined to moving back and forth along this line without changing shape. The criterion for field line intersection is then that the local magnetic field vector lies inside the cone whose apex is at the spacecraft and whose circumference at the base is the locus determined by the tangency points on the hyperboloid (see Figure 1). In a solar ecliptic system that is aberrated and centered at (199.9, −17.7, 0) R_E, the equation of the surface is

$$(X - X_0)^2/a^2 - Y^2/b^2 - Z^2/b^2 = 1$$

where $a = 186.08\ R_E$ and $b = 61.83\ R_E$; the equation reduces for $X_0 = Z = 0$ to an aberrated form of the equation of *Fairfield* [1971]. The reader is referred to Figure 1 of Fairfield's paper, which indicates how well this equation fits the available observations and gives an idea of the frequency of anomalies to be expected. The equation of this surface with $X_0 = 0$ in conventional solar ecliptic coordinates is $Q(X, Y, Z) = 0$, where X, Y, Z are in earth radii, and where $Q(X, Y, Z) = -0.1023X^2 + Y^2 + Z^2 + 0.2012XY + 44.47X - 4.76Y - 629.03$. On each orbit the equilibrium position of this mathematical representation of the bow shock determined by X_0 is adjusted to the last traversal of the shock prior to the interplanetary observations. For the crossings of this data set, $\langle X_0^2 \rangle^{1/2} = 1.96\ R_E$. To be conservative, we require our hit criterion to be met when the field vector is inside a tangent cone to the hyperboloid with X_0 replaced by $(X_0 - 2)$; this situation is equivalent to the bow shock's moving 2 R_E downstream since its last observation. This precaution makes the apex half angle smaller than the tangent cone to the equilibrium surface. Similarly, our miss criterion is met only if the field vector lies outside a tangent cone to the surface with X_0 replaced by $X_0 + 2$. This cone has a wider apex half angle than it would if we had not allowed for shock motion in the criterion.

As the solar wind passes through the bow shock, the direction of bulk flow is deflected from the radial; its direction continues to change as it passes through the sheath. Proton bulk velocity measurements in the magnetosheath are not available on Ogo 5. To transform the observed data into the bulk frame, we adopt the gas dynamic calculations of *Spreiter et al.* [1966] to make the required transformation and to provide a coherent frame for displaying the results. We again assume a bow shock surface cylindrically symmetrical about the aberrated earth-sun line. The angle of deflection and the ratio of postshock to preshock speeds are obtained from the calculations at the corresponding point on the normalized magnetosheath after *Spreiter et al.* [1966] using simultaneous observations made upstream of the earth by MIT plasma instruments on Explorer 33 or 35, kindly supplied by J. Binsack (private communication, 1971). We first normalize the radial distance R at which the shock is observed to standard conditions, using the subsolar magnetopause distance D_1 and the distance D_2 of the bow shock from the earth at the subsolar point. The magnetopause subsolar distance is

$$D_1 = (f^2 H_0^2/k2\pi\rho u^2)^{1/6} \qquad (1)$$

where $H_0 = 0.312$ gauss, k is a factor related to the efficiency of momentum transfer (unity for inelastic collision), and f is the ring current

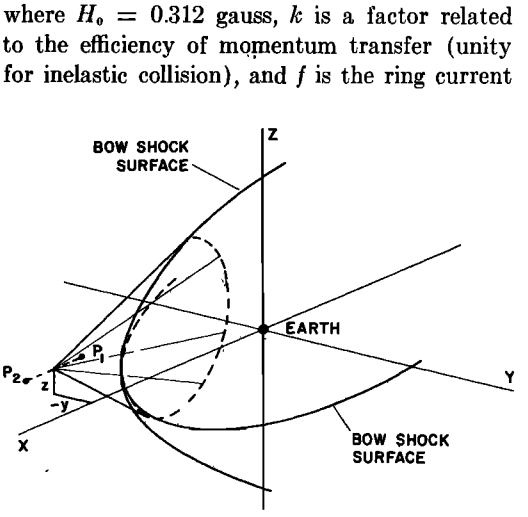

Fig. 1. Illustration of the hit-miss criterion for the interaction of the interplanetary magnetic field with the earth's bow shock. Lines from the position of the instrument (x, y, z) generate a tangent cone to the shock surface. For a hit the direction of the interplanetary field must be inside the tangent cone at P_2.

amplification factor for the standoff magnetopause distance, also taken by Spreiter to be unity. The subsolar shock distance is

$$D_2 = D_1\left[1.1\,\frac{(\gamma - 1)M^2 + 2}{(\gamma + 1)M^2} + 1\right] \quad (2)$$

In these equations, ρ is the mass density, u is the bulk speed upstream, H_0 is the 'standard' earth's field at the nose, γ is the ratio of specific heats taken to be 5/3, and M is the sonic Mach number upstream. The corresponding observations then refer to the point $[R/(D_2), (\Phi - 4.5)]$.

ERRORS

All statistical errors quoted in this paper are defined as $0.67\sigma/N^{1/2}$, where σ^2 is the variance of N observations. The distribution of measurements of $T_\perp$ during our quietest observation period on March 8, 1968, has the lowest dispersion and therefore provides an independent check on our error estimates for the maximum relative error of the temperature. Plotted in histogram form in Figure 2*a* are over 1100 determinations of $T_\perp$ and $T_\parallel$ made while the experiment was in the solar wind on March 8, 1968. For this period the distribution of $T_\perp$ is much narrower than that of $T_\parallel$. The half width for $T_\perp$ is approximately 1.5×10^4 °K, which is ~30% above our estimate of the relative error between measurements from considerations of instrument design. This difference is reasonable when it is interpreted as a contribution due to temporal fluctuations and computational errors in determining $T_\parallel$, $T_\perp$ from the $\{T_{ej}\}$ during the 15-hour observing period. The absolute error estimate $\sim 5 \times 10^4$ °K results from an analysis of the propagation of errors due to counting statistics, convolution, and numerical fits.

INTERPLANETARY OBSERVATIONS

Figure 2*b* is a percentage histogram of electron temperatures T_{ej}, constructed from over 25,000 interplanetary observations, and has a mean value of $1.55 \pm 0.03 \times 10^5$ °K. The temporal average of T_{ej} from all detectors ($\equiv \bar{T}_e$) equals the average of $\frac{1}{3}$ Tr $\mathbf{T}$, if it is assumed that $\mathbf{T}$ has sufficient complexity to represent the thermal state of the plasma. This histogram and the mean electron temperature show excellent agreement with the observations of *Montgomery* [1972]. Although the present observations were made over only 20 days, they cover a wide range of bulk speeds (u = 350–650 km sec^{-1}), a period of interaction between a high-speed stream and slower plasma, and represent a wide variety of solar wind activity. The range of variability of T_{ej} is clearly not as large as that of the proton temperature T_p, which varies over an order of magnitude, as was noted by many workers. Figure 2*c* shows that subset of the data in Figure 2*b* taken on miss field lines, as determined by the criterion discussed above. This subset represents a substantial part of the data in Figure 2*b* and hence its reduced width is significant. The difference between distributions in Figures 2*b* and 2*c* is principally due to the latter's containing a much smaller proportion of temperatures above, say, 1.6×10^5 °K. Although the mean values of these distributions are approximately equal, the miss one is lower in computed value. The temperature measured on hit field lines might be expected to be different from that measured on miss field lines, but this effect might be masked by averaging data over long time periods, and so in Table 1 we examine averages of interplanetary observations by orbit divided into hit and miss categories.

We can see at once from the table that in only one case, orbit 4, do the hit and miss temperatures differ by as much as 1 standard deviation, although in all cases except that of orbit 2 the hit temperature exceeds the miss temperature. In particular, the last column of Table 1 indicates the percentage reliability of the hypothesis that $T_{\text{hit}} = T_{\text{miss}}$. The orbit 4 observations were made close to the leading edge of a high-speed stream. For the first 12 hours of the period the average electron temperature $\bar{T}_e$ remained constant at about 1.65×10^5 °K and rose to about 1.9×10^5 °K during the last 5 hours, during which time the proportion of hits was over 90%, in comparison with 83% for the total observing period. Thus from the present data alone it is not possible to decide whether the temperature increase for this interval is associated with bow shock intersection or with an electron temperature excursion in the solar wind. This time interval will be discussed in more detail below.

Figures 2*a* and 3 illustrate a general feature of our data, namely, that distributions of $T_\perp$

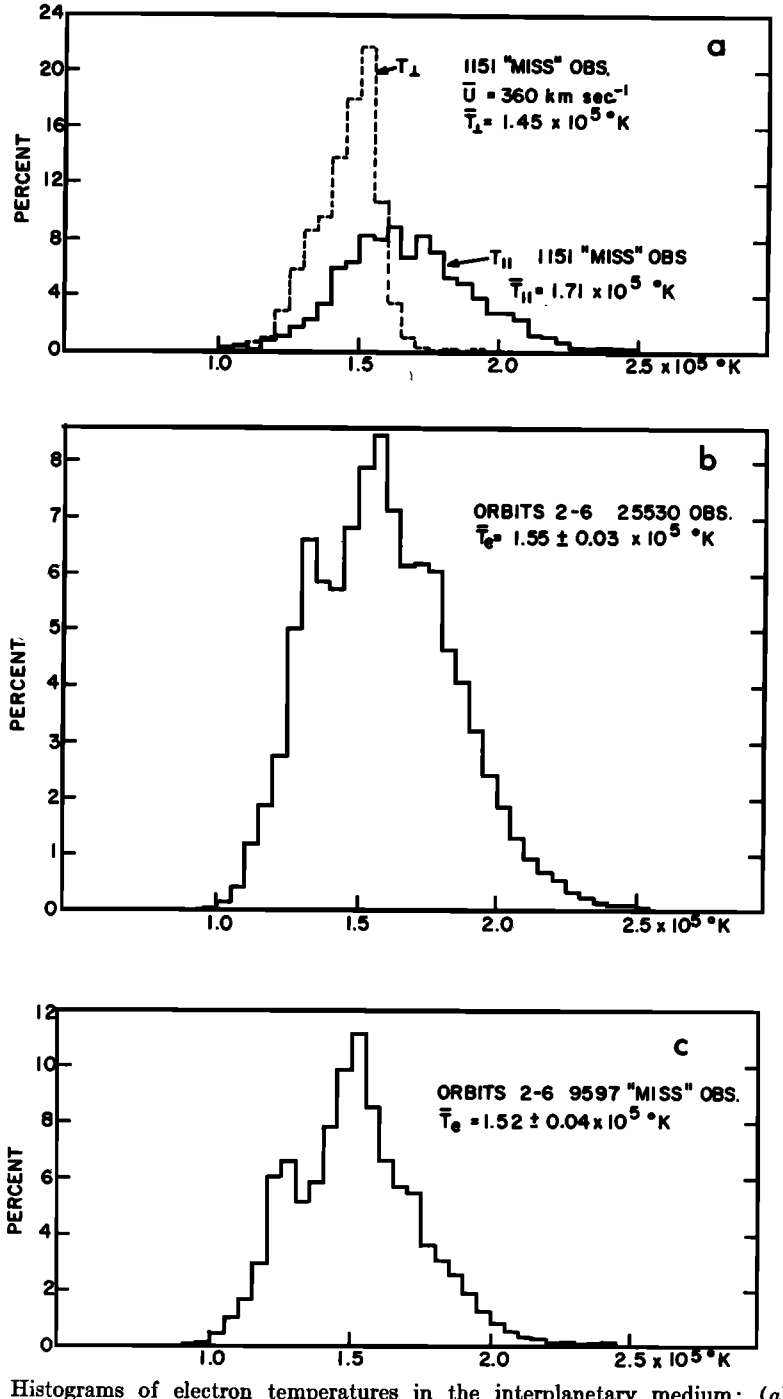

Fig. 2. Histograms of electron temperatures in the interplanetary medium: (*a*) quiet day distribution of $T_\perp$ and $T_\parallel$, (*b*) composite of all electron temperatures T_e during solar wind observations, and (*c*) subset of Figure 2*b* taken on miss field lines in the upstream solar wind.

TABLE 1. Averages of Interplanetary Observations

Orbit	Time Interval,* day: hour	Miss Temperature, 10^5 °K	Number of Data	Hit Temperature, 10^5 °K	Number of Data	Percentage of Reliability $T_{hit} = T_{miss}$
2	68:01–68:16	1.50 ± 0.08	3816	1.45 ± 0.03	687	57
3	70:17–71:09	1.68 ± 0.12	2157	1.75 ± 0.34	3279	85
4	73:07–74:01	1.59 ± 0.02	819	1.71 ± 0.06	4026	28
5	75:14–76:12	1.41 ± 0.04	1314	1.44 ± 0.07	3986	72
6	78:08–79:04	1.37 ± 0.08	1491	1.42 ± 0.07	3955	64

* March 8 = day 68.

are markedly narrower than those of $T_\parallel$. The physical reason for this difference will be discussed below, but here we use this fact to increase the discrimination possible between temperatures on hit and miss field lines. Figure 3*a* shows hit and miss distributions of $T_\perp$ measured on the quietest day of our observations, March 8, between 0300 and 0500 UT and shows the average values of $T_\perp$ on hit and miss lines to be equal. Figure 3*b*, however, from observations taken 18 hours after a sudden commencement, shows a period when the average values of $T_\perp$ characterizing hit and miss field lines differ appreciably. In addition, the distributions are different in shape. The maximum electron energy step used for our temperature fits, that centered at 80 ev, was chosen as a convenient line of demarcation between the velocity distribution of electrons in the solar wind and the distribution of electrons forming the variable high-energy 'tail.' The distribution function does not even approximate a Maxwellian form above about 100 ev. If electron observations at greater than 100 ev are fitted to a Maxwellian distribution, the resulting 'temperature' shows a more obvious dependence on bow shock intersection. For a discussion of this point see the paper by *Ogilvie et al.* [1971], especially Figure 6.

The hit distribution in Figure 3*b* is consistent with the idea that electrons can sometimes travel upstream from the bow shock, on the downstream side of which the differential electron flux, for example, at 45 ev, is typically an order of magnitude greater than that in the solar wind. These higher-energy electrons could augment the flux detected in the higher-energy channels and so raise the temperature deduced from a fit to a Maxwellian velocity distribution function. Higher temperatures on hit field lines might also result from electron heating associated with waves moving upstream from the bow shock. To be detected, electrons originating at or behind the bow shock must travel along the magnetic field line toward the spacecraft while that field line convects from a position first intersecting the shock to a position intersecting the spacecraft. Observations made on the dawn side of the bow shock are favorably situated to detect electrons down to the lowest velocity measured here.

ANISOTROPIES: HIT VERSUS MISS

The electron temperature anisotropy was estimated from 6827 calculations of temperature by the method outlined above and subdivided according to field line geometry. The results were $T_\parallel/T_\perp = 1.24 \pm 0.12$, hit lines (4146 cases), and $T_\parallel/T_\perp = 1.11 \pm 0.18$, miss lines (2681 cases). These results are in good agreement with previous determinations and reinforce the conclusions reached by *Burlaga* [1971] and *Ness et al.* [1971] that the fire hose instability is a rare occurrence in the interplanetary medium. Sometimes negative values of $A' = T_\parallel/T_\perp - 1$ are computed, but these are usually associated with nongyrotropic plasma, and, since such data are therefore not consistent with the hypothesis for determining $T_\parallel/T_\perp$, they have been omitted.

EVIDENCE FOR ELECTRON TEMPERATURE GRADIENT

A large density peak occurred at 0600 UT on March 14, and the rise in bulk speed to 650 km sec^{-1} started at 0500 UT and peaked about 24 hours later. Proton temperatures (J. Binsack, private communication, 1971) rose simultane-

ously with the bulk speed. These are common indicators of the interaction of a high-speed stream with the ambient plasma [*Siscoe*, 1972; *Gosling et al.*, 1972]. In this case, however, a compression of density from about 10 to 50 cm^{-3} was observed, which is larger than the 'typical' enhancement described by *Gosling et al.* [1972], i.e., 3:1. Before the most rapid increase of density, hourly average electron and proton temperatures showed marked

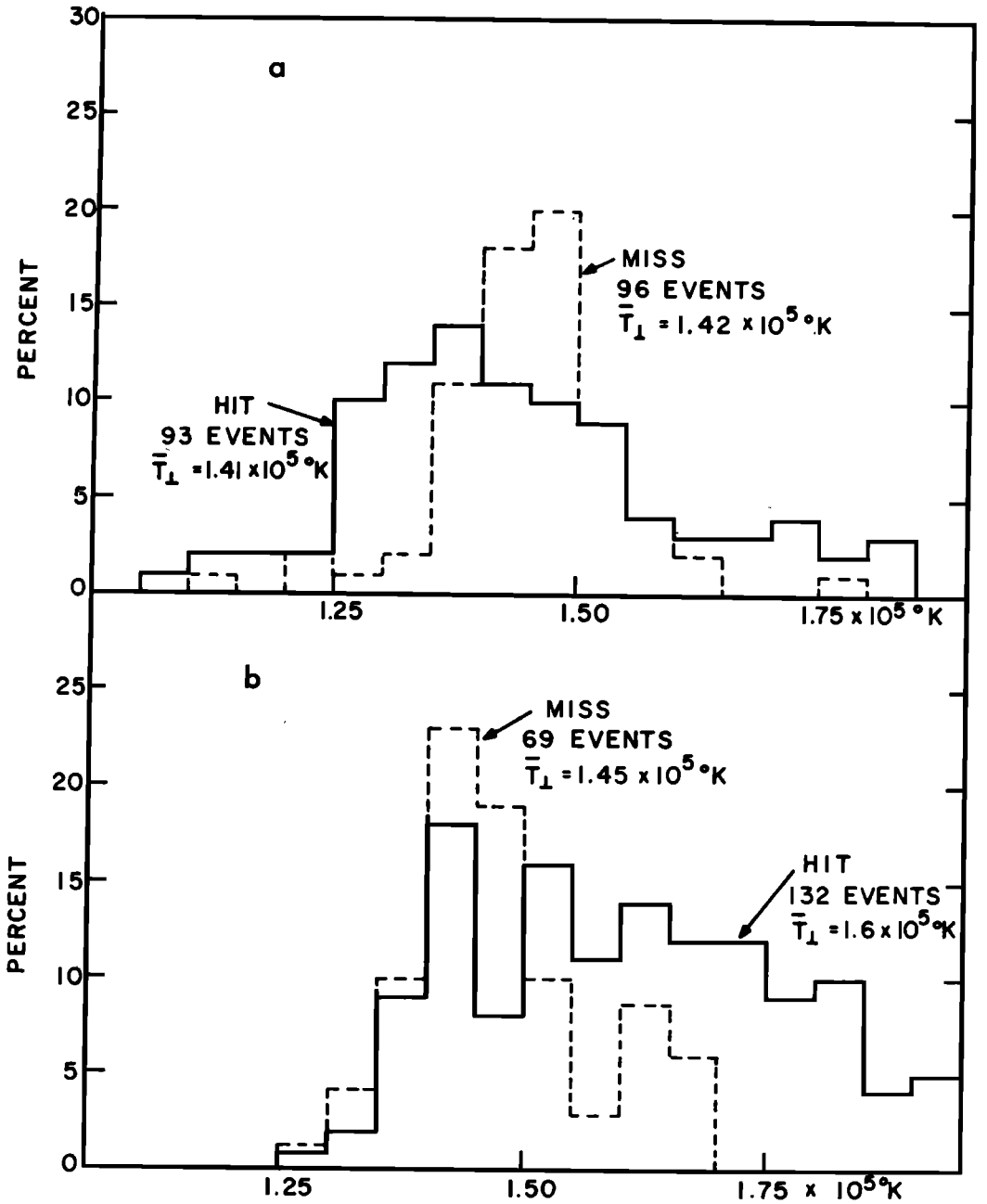

Fig. 3. Perpendicular temperatures on hit and miss magnetic field lines for (*a*) March 8, 1968, 0300–0500 UT, and (*b*) March 10, 1968, 1800–2000 UT.

gradients (Figure 4). The change in electron temperature from 1.65×10^5 to 1.9×10^5 °K in a period of about 7 hours took place before the proton temperature rise usually accompanying a bulk speed increase.

The convective derivative of the electron temperature has the form

$$dT_e/dt = \partial T_e/\partial t + V \cdot \nabla T_e$$

If long-time (macroscale) changes associated with the corona are neglected,

$$\left.\frac{dT_e}{dt}\right|_{\text{obs}} (\text{mesoscale}) = \frac{\partial T_e}{\partial t} + V \cdot \nabla T_e \quad (\text{mesoscale}) \qquad (3)$$

In a coordinate system in which the Z axis is along $\mathbf{B}$, the Y axis is perpendicular to the ecliptic, and the X axis forms a right-hand triad, the solar wind vector observed may be represented as V_{sw} $(2/2^{1/2}, 0, 2/2^{1/2})$. Equation 3 then becomes

$$\left.\frac{dT_e}{dt}\right|_{\text{obs}} = V_{sw} \frac{2^{1/2}}{2}\left[\frac{\partial T_e}{\partial x} + \frac{\partial T_e}{\partial z}\right] + \frac{\partial T_e}{\partial t} \qquad (4)$$

The present observations were taken close to the interface between colliding streams, and such structures evolve on the macro time scale, even though the interface is on the mesoscale. We assume constancy of conditions during our measurements in the gradient region and ignore the last term of (4). A calculation of the relaxation time for electron hot spots in the solar wind has been made by *Hundhausen and Montgomery* [1971], corresponding to a value of $(1/T_e)\ dT_e/dt$ of 15% per day. The observed value of $(1/T_e)\ dT_e/dt$ is ~65% per day, more than 4 times that calculated by *Hundhausen and Montgomery* [1971] for a transient relaxation process, and thus the present observations are shown to be of a steady state. We conclude our observation to be of a spatial electron temperature gradient convected past the detector.

The existence of 'cold' electron regions, with $T_e \simeq 5 \times 10^4$ °K reported by *Montgomery et al.* [1972], indicates that electron temperature gradients occur, but gradients as steep as the present one might be expected to have been observed relatively rarely because of both their magnitude and the short time of continuous observations of solar wind electrons presented to date. The data also show that $\bar{T}_e$, the hourly average of each set of values of T_e from the three orthogonal detectors, does not fall between $T_\perp$ and $T_\parallel$, as it should if the plasma is gyrotropic. A plasma exhibiting energy transfer via collective processes across the field is nongyrotropic.

Velocity Distribution Function in the Magnetosheath

Figure 5 shows typical empirical velocity distribution functions in the interplanetary medium and in the sheath adjacent to a bow shock crossing. At low velocities the interplanetary measurements show no gross distortions, the tail at high velocities beginning to show up in Figure 5 detector 1 has been exhibited and discussed by *Ogilvie et al.* [1971].

Because of the preacceleration of electrons used in this detector, the energy channel centered at 10 ev (1900 km sec^{-1}) covered the electron energy range from 1.2 to 18.8 ev and the 25-ev channel from 15 to 35 ev. The increased flux measured at 10 ev and absent at 25 ev when in the sheath represents electrons with energies between 1.2 and 15 ev measured in the magnetosheath but not in the solar wind. We assume that these data result either from a small shift in spacecraft potential or from the increased flux of secondary electrons from the spacecraft produced by the increased flux of electrons with energies of ~100 ev in the sheath or a combination of both effects. In our analysis of data taken in the sheath we have not included the 10-ev point in the empirical distribution function but have extrapolated to zero velocity from the 25-ev level; this procedure introduces negligible error because of the form of the moment integrals near the origin.

The sheath distribution function shows the flat-topped form previously noted by *Montgomery et al.* [1970]. This function characterizes the sheath between 6.4 and 7.6 hours LT along the orbits, although the extent of the velocity range showing a flat top varies with position. This form is no more than marginally stable, and its presence in the region explored by this experiment illustrates the nonequilibrium nature of the magnetosheath.

As can be seen at once from Figure 5, the

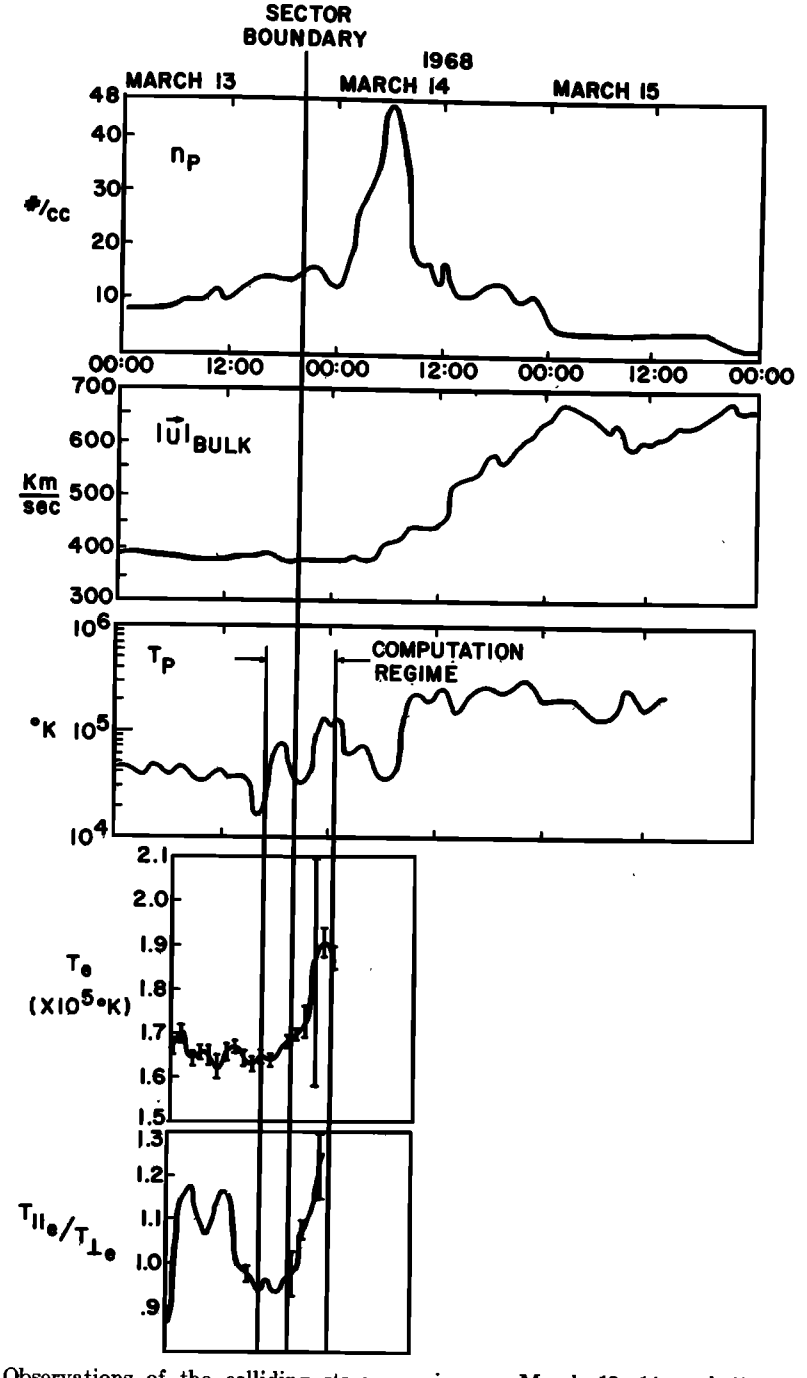

Fig. 4. Observations of the colliding stream region on March 13, 14, and 15, 1968. The proton density n_p, U_p, and T_p data from Explorer 35 are used with the permission of J. Binsack.

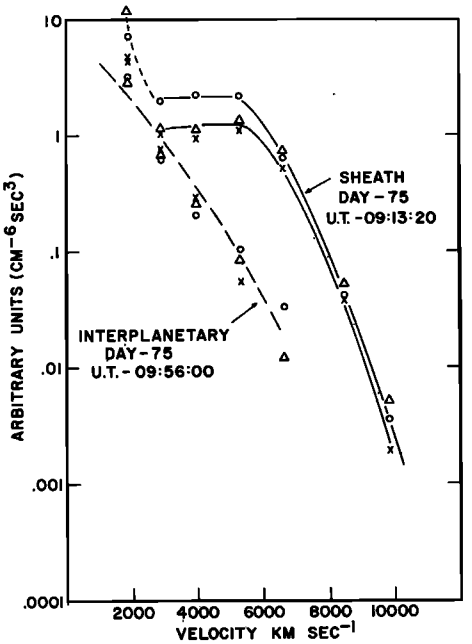

Fig. 5. Empirical velocity distribution function in arbitrary units for the magnetosheath contrasted with similar measurements in the magnetosheath. Detector 1 is indicated by circles, detector 2 by triangles, and detector 3 by crosses.

empirical distribution function obtained up to velocities of $\simeq$6000 km sec^{-1} by one detector differs by about 80% from the functions obtained by the other two, whereas 13 min later all three detectors agreed to within $\pm$20% in the solar wind. The detectors had been intercalibrated by means of the method discussed by *Ogilvie et al.* [1971], and, since these are empirical velocity distribution functions in the frame moving with the plasma, convective effects have been removed.

In deriving f from the observed fluxes an error could be caused by assigning an incorrect bulk speed in the sheath. Since $\partial f/\partial\omega$ is approximately zero between 3000 and 6500 km sec^{-1}, the maximum percentage error in f can be calculated by differentiating the expression

$$f = F\left\{\omega_u^4\left[1 + \frac{2u}{\omega_u} + \frac{u^2}{\omega_u^2}\right]^2 - \omega_L^4\left[1 + \frac{2u}{\omega_L} + \frac{u^2}{\omega_L^2}\right]\right\}^{-1}$$

where F denotes flux and ω_u and ω_L are the upper and lower random velocity limits given above and, to give the maximum effect, u is assumed directed toward the sun. If terms in u^3/ω_u^3 and u^3/ω_L^3 are neglected, the result is that a 100-km sec^{-1} error in bulk speed is required to give a 10% error in f in the lowest energy range, whereas the discrepancy between the detectors is constant at a value of about 80%, independent of velocity. This discrepancy is thus not due to the detectors or to an incorrect assignment of the bulk speed frame but represents a real physical effect, which we associate with energy conduction in the magnetosheath.

Our observations cannot demonstrate, but are consistent with, flow along a radius vector toward the earth. Because of the turbulent nature of the magnetosheath flow field illustrated below, it is unlikely that the energy flow would be confined to the direction of the local magnetic field but rather would be in the direction of the temperature gradient.

During the operation of this experiment, 34 bow shock crossings were observed for which stable observations on both sides of the shock were available. Temperatures and densities in the solar wind were obtained by fitting the observations to a convected Maxwellian velocity distribution as described before. In the sheath, kinetic densities and temperatures were calculated from the moments of the empirical distribution function determined by the three detectors, extrapolated to zero velocity excluding the point at 1900 km sec^{-1}, as is discussed above. Figure 6 shows histograms of the 34 observed density and temperature ratios across the shock. The average density increase is 2.1:1, and the average temperature increase is 4.2:1. The density increase is distributed in a narrow range about the mean, but the temperature increase is more widely distributed and shows a tendency to increase with increasing solar wind Mach number. These values, obtained for a variety of conditions, are consistent with those given by *Hundhausen* [1970] and *Montgomery et al.* [1970] for quiet conditions of 3:1 for the density and 3.3:1 for the temperature. In particular, the temperatures shown by *Hundhausen* [1970] for measurements made on

February 4, 1967, agree well with the present results both in magnitude and in range.

MAGNETOSHEATH TEMPERATURE AND DENSITY VARIATIONS

Since we have used the hydromagnetic theory of *Spreiter et al.* [1966] to normalize our data with respect to the position of the bow shock and upstream conditions using Explorer 33 and 35 plasma data, it is of interest to see whether this theory can be used to interpret and organize our data in the magnetosheath. The accuracy to be expected is not high, because of the variability of conditions during each pass, but we have examined our observations of density and temperature along the path of the spacecraft through the magnetosheath. We expect a decrease in temperature of about 15% and an increase in density of about 30% as the spacecraft goes from the magnetopause to the bow shock. We have used the theory to normalize the position of the spacecraft with respect to the magnetosphere and shock and to transform into the random frame of the plasma; therefore the present observations do not constitute an independent test of the theory but simply a consistency check. The density and temperature are not strongly dependent on the choice of γ. In Figure 7 we show temperature estimates and normalized density observations for three passes through the magnetosheath. No regularity in the density observations can be seen as a result of large density fluctuations everywhere in the magnetosheath. For the temperature observations the solid lines indicate the approximate gradients to be expected on the Spreiter model as one goes from the empirically determined position of the magnetopause to that of the shock. The dotted line is the predicted bow shock position given by theory for $\gamma = 5/3$ and $f^2/k = 1$, as used by Spreiter. We see that our temperature gradients are in reasonable agreement with theoretical predictions for two of the three cases but that the theory predicts a bow shock much closer to the earth than that observed.

The parameters available to modify these predictions are γ and f^2/k. If $[\Delta(R/D_2)]/(R/D_2)$ is a small fractional change in R/D_2 as a result of changes in f^2/k and γ and R is the point of observation, we can write

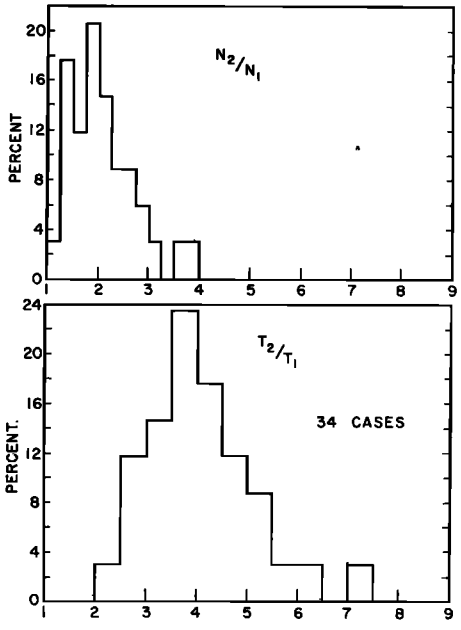

Fig. 6. Histograms of electron density and temperature ratios for the 34 bow shock crossings observed.

$$\frac{\Delta(R/D_2)}{R/D_2} \simeq \frac{1}{R/D_2} \cdot \left[\frac{\partial}{\partial D_1}\left(\frac{R}{D_2}\right)\Delta D_1 + \frac{\partial}{\partial \gamma}\left(\frac{R}{D_2}\right)\Delta\gamma\right] \quad (5)$$

Schield [1969] has published a tabulation of values of f^2/k, which indicates a weak dependence of this quantity on γ, but in view of the $\frac{1}{6}$ power dependence in (1) we can write

$$\frac{\Delta(R/D_2)}{R/D_2} \simeq -\frac{\Delta D_1}{D_1} - \frac{9}{40}\frac{\Delta\gamma}{\gamma}$$

In Table 2 we show the results of observations from the three passes through the magnetosheath. Bearing in mind that (5) represents an expansion about the value $\gamma = 5/3$ and neglects nonlinear effects, approximate contributions to $\Delta(R/D_2)/(R/D_2)$ are given. The quiet time ring current contribution shown in the third column will not account for any of the observed change in R/D_2. The first observations, showing a large discrepancy, were made at a very quiet time, whereas the third set, made on March 15, 1968, was at a time when the earth was immersed in a high-speed stream. These conditions

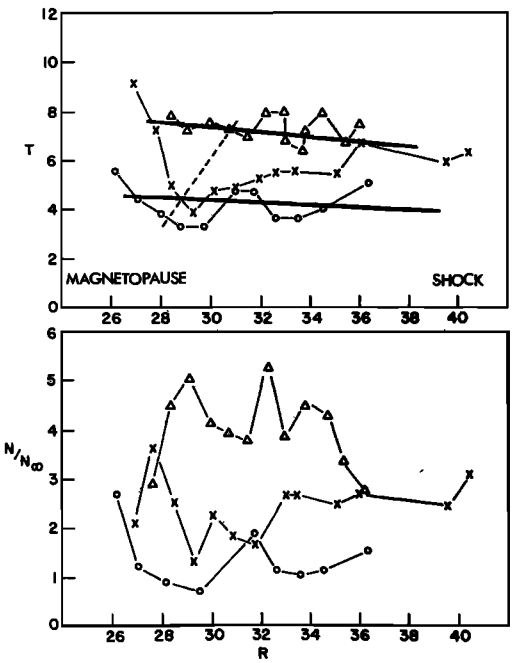

Fig. 7. Electron temperature and density variations observed during three traversals of the magnetosheath on March 7 (circles), March 12 (crosses), and March 15 (triangles), 1968; T is in units of 10^5 °K and R is in arbitrary units. Dashed line shows expected variation [after *Spreiter et al.*, 1966]. Connected symbols are successive intervals in normalized radial distance at a fixed normalized angle from the aberrated subpolar point.

can be reconciled with theory by a modest storm time ring current.

A reduction in the value of γ below 5/3, as previously suggested to reflect the increase in the number of available degrees of freedom provided by turbulent motion in the sheath, increases the discrepancy noted here by reducing the standoff distance of the shock. As a consequence of the motion of the sonic line with change in Mach number, the observations on March 15 were probably taken in a subsonic plasma, whereas the more discrepant observations were probably made in a trans-sonic plasma with somewhat more restricted degrees of freedom. This effect acts in the correct direction to provide a qualitative explanation of the results, but detailed calculations would be required to test it quantitatively. In view of the time variations superposed on the spatial variations discussed here these tests have not been carried out.

CONCLUSIONS

The distribution in Figure 2*b* shows the electron temperature to remain between 1.0 and 2.5 × 10^5 °K over the wide range of solar wind conditions sampled during our investigation. We have demonstrated that the distribution of $T_\perp$ is narrower than that characterizing $T_\parallel$ (e.g., Figure 2*a*) and that this difference is a general property of our data. We suggest that this is a consequence of the adiabatic invariance of the magnetic moment of the electrons

$$\mu_\perp = \tfrac{1}{2} m_e v_\perp^2 / B$$

where $\frac{1}{2}m_e v^2 = \frac{1}{2}m_e(v_\perp^2 + v_\parallel^2)$ in spatially inhomogeneous and time dependent fields and that changes in electron temperature show up as larger changes in $T_\parallel$ than in $T_\perp$.

This conclusion is supported by Figure 8, in which we show a typical plot of $T_\perp/|B| \simeq \mu_\perp$ and $T_\parallel/|B| \simeq \mu_\parallel$, for miss conditions. The distribution of the adiabatic invariant $\mu_\perp$ is narrower than that of the analogously defined expression $\mu_\parallel$, which is of course not conserved.

We have divided our interplanetary data into a part taken on magnetic field lines that intersect a model of the earth's bow shock and a part taken on nonintersecting field lines. Although an

TABLE 2. Results of Observations from the Three Passes through the Magnetosheath

Date 1968	$\frac{\Delta(R/D_2)\text{ Measured}}{R/D_2\text{ Theory}}$	Estimate* of Ring Current Changes $\frac{\Delta(R/D_2)}{R/D_2}$	Residual $\frac{\Delta(R/D_2)}{R/D_2}$	$\frac{\Delta\gamma}{\gamma}$ Required To Remove Residual	M_∞
March 7	−0.37	−0.08	−0.29	1.28	7
March 12	−0.39	−0.08	−0.31	1.37	~8
March 15	−0.15	−0.08	−0.07	0.31	~11

* Quiet time ring current.

electron temperature difference between these sets of observations might be expected, we have shown that its magnitude, as observed in our data, averaged over periods of hours approaches our level of precision of about 3%. This statement applies to temperatures determined from observations below 95 ev. We have observed times when the value of $T_\perp$ on hit lines exceeds that on miss lines by ~10%, so there certainly are times when intersecting magnetic field lines have an increased population of electrons of energy of the order of 100 ev.

Observed distribution functions for electrons in the whole region of the magnetosheath investigated here have the flat-topped form previously observed by Vela spacecraft in a different spatial region. This implies that the plasma in this region is not in equilibrium. Using temperatures and densities derived from these observed distribution functions, we have shown that the average density ratio across the bow shock is ~2:1 in this position, where the average interplanetary magnetic field meets the bow shock approximately parallel to its normal. We have also generally observed the electron distribution function in the magnetosheath to be asymmetrical about the direction perpendicular to the satellite-earth line. This result is consistent with energy transport in the sheath, but the present observations were made from an attitude-stabilized spacecraft, and thus a precise determination of the net flux and its direction is impossible. Quasi-steady assumptions regarding the solar wind electron distribution used previously to determine heat fluxes [*Ogilvie et al.*, 1971] cannot be extended to the sheath because the time scale of the turbulence has not been established. We point out, however, that the only presently reported test of the Rankine-Hugoniot equations at the bow shock [*Mariani et al.*, 1970] with an overdetermined set of observed parameters required an energy flux in the sheath to predict the measured density jump [*Howe*, 1970].

Temperature and density observations along three passes through the magnetosheath do not consistently fit the predictions of the hydromagnetic theory, even when the effects of possible variations of γ, quiet time ring currents, variations in the nature of the momentum transfer at the magnetopause, and upstream conditions are all taken into account.

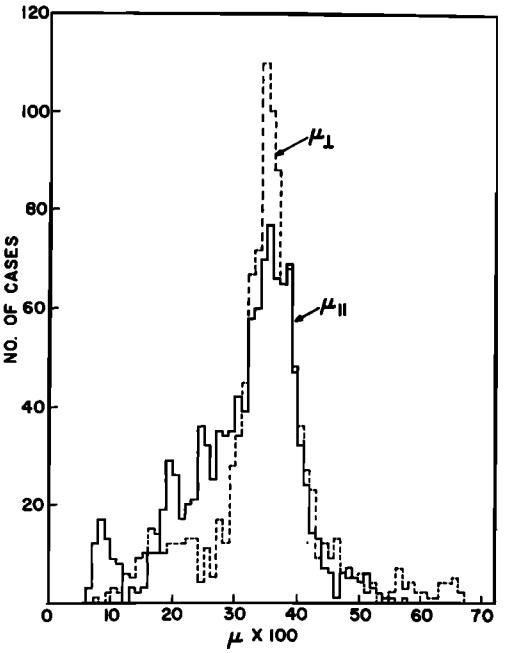

Fig. 8. Distribution of $mv_\perp^2/B$ and $mv_\parallel^2/B$ for the period 01h 00m 19s to 15h 30m 28s UT, March 8, 1968.

Acknowledgments. We wish to acknowledge the contributions of Dr. Wilkerson of the University of Maryland to the design and calibration of the instrument and thank Drs. J. P. Heppner and M. Sugiura for permission to use the Ogo 5 magnetic field data.

* * *

The Editor thanks S. J. Bame and A. J. Hundhausen for their assistance in evaluating this paper.

REFERENCES

Asbridge, J. R., S. J. Bame, and I. B. Strong, Outward flow of protons from the earth's bow shock, *J. Geophys. Res.*, *73*, 5777, 1968.

Burlaga, L. F., Hydromagnetic waves and discontinuities in the solar wind, *Space Sci. Rev.*, *12*, 600, 1971.

Fairfield, D. H., Bow shock associated waves observed in the far upstream interplanetary medium, *J. Geophys. Res.*, *74*, 3541, 1969.

Fairfield, D. H., Average and unusual locations of the earth's magnetopause and bow shock, *J. Geophys. Res.*, *76*, 6700, 1971.

Frank, L. A., and W. L. Shope, A cinematographic display of observations of low-energy proton and electron spectra in the terrestrial magnetosphere and magnetosheath and in the interplanetary medium (abstract), *Eos Trans. AGU*, *49*, 279, 1968.

Fredericks, R. W., F. L. Scarf, and L. A. Frank, Nonthermal electrons and high-frequency waves in the upstream solar wind, *J. Geophys. Res.*, *76*, 6691, 1971.

Gosling, J. T., A. J. Hundhausen, V. Pizzo, and J. R. Asbridge, Compressions and rarefactions in the solar wind: Vela 3, *J. Geophys. Res.*, *77*, 5442, 1972.

Howe, H. C., Pioneer 6 plasma measurements in the magnetosheath, *J. Geophys. Res.*, *75*, 2429, 1970.

Hundhausen, A. J., Plasma measurements across the bow shock and in the magnetosheath, in *Intercorrelated Satellite Observations Related to Solar Events*, edited by V. Manno and D. E. Page, p. 155, D. Reidel, Dordrecht, Netherlands, 1970.

Hundhausen, A. J., and M. D. Montgomery, Heat conduction and nonsteady phenomena in the solar wind, *J. Geophys. Res.*, *76*, 2236, 1971.

Lind, D. L., and N. McIlwraith, Plasma electron detector using an open electron multiplier, *Trans. Nucl. Sci.*, *18*, 511, 1966.

Mariani, F., B. Bavassano, and N. F. Ness, Magnetic field fluctuations observed in the magnetosheath by Pioneer 7 and 8, *J. Geophys. Res.*, *75*, 6037, 1970.

Montgomery, M. D., Average thermal characteristics of solar wind electrons, Solar Wind, *Nasa Spec. Publ. 308*, p. 208, 1972.

Montgomery, M. D., S. J. Bame, and J. R. Asbridge, Solar wind electron Vela 4 measurements, *J. Geophys. Res.*, *73*, 4999, 1968.

Montgomery, M. D., J. R. Asbridge, and S. J. Bame, Vela 4 plasma observations near the earth's bow shock, *J. Geophys. Res.*, *75*, 1217, 1970.

Montgomery, M. D., J. D. Asbridge, S. J. Bame, and W. C. Feldman, Positive evidence for closed magnetic structures in the solar wind associated with interplanetary shock waves (abstract), *Eos Trans. AGU*, *53*, 503, 1972.

Ness, N. F., A. J. Hundhausen, and S. J. Bame, Observations of the interplanetary medium: Vela 3 and Imp 3, 1965–1967, *J. Geophys. Res.*, *76*, 6643, 1971.

Ogilvie, K. W., J. D. Scudder, and M. Sugiura, Electron energy flux in the solar wind, *J. Geophys. Res.*, *76*, 8165, 1971.

Schield, M. A., Magnetosphere pressure balance, *J. Geophys. Res.*, *74*, 1275, 1969.

Scudder, J. D., The transfer function of the Ogo-5 electron spectrometer and other similar preaccelerating particle spectrometers, internal technical document, NASA/GSFC, Greenbelt, Md., 1972.

Serbu, G. P., Explorer 35 observations of solar wind electron density, temperature, and anisotropy, *J. Geophys. Res.*, *77*, 1703, 1972.

Siscoe, G. L., Structure and orientations of solar wind interaction fronts: Pioneer 6, *J. Geophys. Res.*, *77*, 27, 1972.

Spreiter, J. R., A. L. Summers, and A. Y. Alksne, Hydromagnetic flows around the magnetosphere, *Planet. Space Sci.*, *14*, 223, 1966.

Wolfe, J. H., and D. D. McKibben, Pioneer 6 observations of a steady state magnetosheath, *Planet. Space Sci.*, *16*, 953, 1968.

Wolfe, J. H., R. W. Silva, and D. D. McKibben, Pioneer 6 observations of plasma ion and electron heating at the earth's bow shock (abstract), *Eos Trans. AGU*, *48*, 174, 1967.

(Received November 28, 1972;
accepted March 29, 1973.)